Accepted Manuscript

Enhanced Electrocatalytic Performance of Co_3O_4/Ketjen-Black Cathodes for Li-O_2 Batteries

Dan Zhang, Baoqi Wang, Yinzhu Jiang, Peng Zhou, Zhihui Chen, Ben Xu, Mi Yan

PII: S0925-8388(15)31044-6

DOI: 10.1016/j.jallcom.2015.09.068

Reference: JALCOM 35343

To appear in: *Journal of Alloys and Compounds*

Received Date: 28 July 2015

Revised Date: 3 September 2015

Accepted Date: 8 September 2015

Please cite this article as: D. Zhang, B. Wang, Y. Jiang, P. Zhou, Z. Chen, B. Xu, M. Yan, Enhanced Electrocatalytic Performance of Co_3O_4/Ketjen-Black Cathodes for Li-O_2 Batteries, *Journal of Alloys and Compounds* (2015), doi: 10.1016/j.jallcom.2015.09.068.

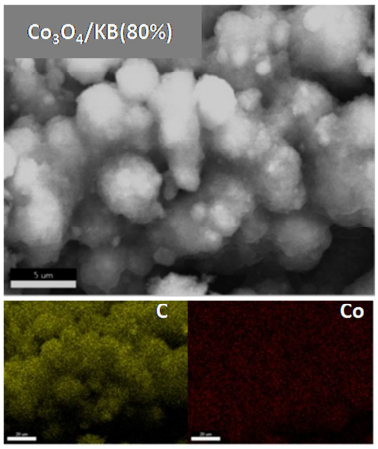

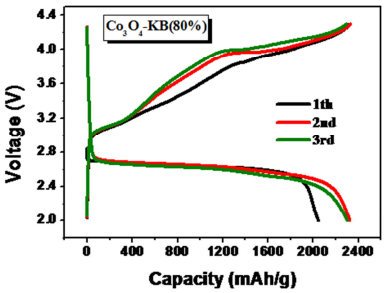

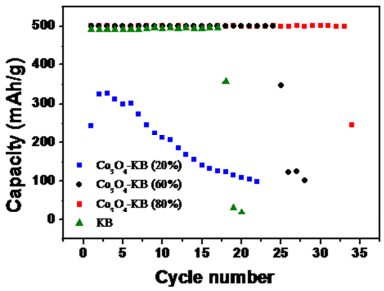

Enhanced Electrocatalytic Performance of Co_3O_4/Ketjen-Black Cathodes for Li-O_2 Batteries

Dan Zhang [a,†], Baoqi Wang [a,†], Yinzhu Jiang [a,], Peng Zhou [a], Zhihui Chen [a], Ben Xu [b], Mi Yan [a,*]*

[a] *State Key Laboratory of Silicon Materials, Key Laboratory of Novel Materials for Information Technology of Zhejiang Province and School of Materials Science and Engineering, Zhejiang University, Hangzhou, Zhejiang 310027, P. R. China*

[b] *Smart Materials and Surfaces Lab, Mechanical Engineering, Faculty of Engineering and Environment, Northumbria University, Newcastle upon Tyne, NE1 8ST, UK*

[†] *These authors contributed equally.*

* Correspondence author: yzjiang@zju.edu.cn (Y.Z. Jiang); mse_yanmi@zju.edu.cn (M. Yan)

Abstract

A series of Co_3O_4/Ketjen Black cathodes are fabricated by electrostatic spray deposition technique for Li-O_2 batteries. A sluggish kinetics of oxygen reduction reaction and oxygen evolution reaction processes is noted either when Co_3O_4 is lacked or Ketjen Black is insufficient, which leads to much higher overpotentials between charge and discharge profiles. By contrast, with the optimal design in terms of electric conduction and catalytic activity, the Co_3O_4/Ketjen Black (80 wt%) composite achieves enhanced electrochemical performance with an initial discharge capacity of 2044 mAh g^{-1} and maintaining 33 cycles at a fixed capacity of 500 mAh g^{-1}. The electrochemical characterization indicates that the improved Li-O_2 battery performance may benefit from the highest oxygen reduction reaction and oxygen evolution reaction activity under this electro-chemically optimized composite. This work may shed light on the design principle of future cathode materials for Li-O_2 batteries.

Keywords: lithium-oxygen battery; cobalt oxide; electrostatic spray deposition; electrical conductivity; catalytic activity.

1. Introduction

Rechargeable lithium-oxygen (Li-O_2) battery has been considered as a promising alternative to lithium-ion battery (LIB) in the application fields of vehicle electrification and large-scale energy storage, owing to its higher (~3 to 5 times) practical gravimetric energy density [1-3]. However, the proposed replacement by Li-O_2 batteries still faces several technical challenges such as large voltage hysteresis, low round-trip efficiency and short cycle life [4-6]. Intensive research efforts towards better understanding of oxygen reduction reaction (ORR) and oxygen evolution reaction (OER) mechanisms, and the design principles of highly efficient ORR & OER catalysts are critical in improving battery performance [7-10]. Different from the intercalation mechanism in LIBs, Li-O_2 batteries are based on an electrocatalytic mechanism for both ORR and OER processes, where “electro” emphasizes the essentially smooth transportation for electrons, and “catalytic” indicates the necessity of catalysts with intrinsically high activity. A well-known discharge reaction in a stable Li-O_2 battery is the formation of lithium peroxide on the surface of cathode where oxygen reacts with lithium ions and electrons, $2Li^{+}+O_2+2e^{-}\rightarrow Li_2O_2$ [11-14]. Both the electric conductivity and catalytic activity play important roles to avoid sluggish kinetics of in ORR process. The OER process follows the same rule as well.

It is necessary to investigate the relationship between catalytic activity and electric conduction in the electrocatalytic processes. Two primary kinds of cathode catalysts have been proposed in the previous research on Li-O_2 batteries: noble metals and

transition metal oxides. Noble metals (such as nanoporous Au[15], PtAu nanoparticles[16], Ru nanocrystals[17]) are not ideal in this study not only because of the impractical cost but also their sufficient conductivity. Transition metal oxides especially Co_3O_4, however, has attracted considerable interests as a promising catalyst for its low cost and outstanding catalytic activity [18-22]. Bruce *et al.* reported a series of oxide catalysts for non-aqueous Li-O_2 cells. Among the oxide catalysts studied by far, Co_3O_4 gives the best compromise between initial capacity and capacity retention as well as the lowest charging voltage of 4.0 V [23]. Since Co_3O_4 is poor in electronic conduction, so the typical strategy was to be mixed with porous carbon materials for catalytic reaction [20, 24-26]. Ketjen Black (KB) is one of the most favorable conductive agents among carbon black in Li-O_2 batteries for its low cost, superior specific surface area and ultrahigh electric conductivity. In this work, we propose a prototype cathode of Co_3O_4/KB composites, in which Co_3O_4 behaves mainly as a pure catalyst while KB plays as conductive agent, to study the relationship of catalytic function and electric conduction for the optimized electrocatalytic effect in Li-O_2 batteries.

Co_3O_4/KB composites were fabricated in one-pot by a facile electrostatic spray deposition (ESD) technique. We optimized the performance of the composites through adjusting electric conductivity and catalytic activity with different weight ratios of Co_3O_4 to KB. Benefitted from the lowest electrochemical impedance and adequate catalytic activity, the Co_3O_4/KB(80%) electrode exhibits the highest Li-O_2 battery performance, exhibiting the lowest overpotential of less than 1.0 V at 100 mA g^{-1}, and

the most stable cyclability of 33 cycles with the limitation of the capacity to 500 mA h g^{-1}.

2. Experimental

2.1.Synthesis of the Co_3O_4/KB cathodes

Co_3O_4/KB porous films were directly deposited on foam Ni by ESD technique. The $Co(acac)_2$ precursor was pre-dissolved in 1,2-propylene glycol (0.01 mol L^{-1}). Different weight of KB was further added into the prepared $Co(acac)_2$ solution under continuous stirring. The liquid feedstock was pumped at a feeding rate of 2 ml h^{-1} into a stainless steel nozzle (inner diameter, 0.8 mm) followed by electrostatic atomization (~12 kV, DC voltage) and a subsequent deposition on a heated substrate. The distance between the nozzle and the substrate was fixed at 4 cm, whereas the substrate temperature was kept at 230 ^oC. As for fabricating pure KB cathode, a mixture slurry with a weight percentage of 90% KB and 10% PTFE binder was prepared and then coated onto the Ni-foam substrate, followed by a drying process in a vacuum oven at 80 ^oC for 12h. The mass loading of O_2 electrodes was measured using a microbalance with an accuracy of 0.002mg (Sartorius CPA26P, Germany) before and after deposition. A series of cathodes of pure Co_3O_4, Co_3O_4/KB (20%), Co_3O_4/KB (60%) and Co_3O_4/KB (80%) were prepared. The percentage in bracket after KB means the weight ratio of KB in this composite.

2.2. Li-O_2 cell assembly

Li-O_2 coin cells were assembled in an argon-filled glove box to ensure an isolating atmosphere with both the moisture and oxygen concentration less than 1 ppm. The

positive top cover of type 2025 coin cell was pre-machined by drilling 7 evenly distributed 1.5 mm diameter holes to enable oxygen flow. Lithium foil was used as both counter and reference electrode, and a glass fiber separator (Whatman GF/D microfiber filter paper, 2.7 um pore size) was used to absorb enough electrolytes to prevent electrolyte evaporation in an open environment. The electrolyte consisted of 1 M LiTFSi (>98%, Alfa) in triethylene glycol dimethyl ether (TEGDME, >99%, Sigma-Aldrich). The as-prepared air cathode was dried at 110 ^{o}C in a vacuum oven for 12 h. After the assembly, the cells were transferred to a sealed glass box filled with 1 atm high-purity oxygen. All the specific capacities of Li-O_2 battery were calculated based on the mass of total cathode materials.

2.3. Sample characterization

X-ray Diffraction tests were conducted on Shimadzu XRD-6000 with Ni-filtered Cu Kα radiation (λ=1.5406 Å) at a voltage of 40 kV and a current of 40 mA. FESEM images were acquired at Hitachi S-4800 microscope operated at 5 kV. XPS measurements were performed on Escalab250 X-ray photoelectron spectrometer with a standard Al Kα source (1486.6 eV). The charge/discharge tests were performed on a multichannel battery tester (NEWWARE, BST-610). Cyclic voltammetry (CV) tests were conducted on a CHI660C electrochemistry workstation between 2.0 and 4.3 V (vs Li/Li^{+}) at a scan rate of 0.5 mV s^{-1}.

3. Results and discussion

We firstly observe the morphologies of the obtained samples, as shown in Fig. 1a, the as-deposited pure Co_3O_4 presents an interconnected network structure with many

bowl-like particles embedded with size distribution of 100-200 nm. For the composites with 20% of KB, there shows a trend of aggregation into carbon clusters (Fig. 1b), the bowl-like Co_3O_4 particles on the surface of clusters could be still seen from the enlarged SEM image in the inset of Fig. 1b. When the KB concentration further increases, we observed that the KB nanoparticles may fill in the bowls of Co_3O_4 to generate a slightly denser morphology as shown in Fig. 1c (60% KB) and Fig. 1d (80% KB). The pure KB cathode exhibits a similar loose feature (Fig. 1e) which insures all cathode materials are mainly different in the percentage of KB while excluding the influence of morphology. In the meantime, as a whole Co_3O_4 and KB are homogeneously mixed for different samples as the EDS maps of C and Co demonstrate (Fig. 2). The rough sketch of the EDS maps of C match well with the carbon clusters from the original SEM images, while the EDS maps of Co seems more uniform in whole view, which means Co_3O_4 are more uniformly distributed.

XRD pattern (Fig. 3a) of the as-prepared Co_3O_4 film clearly reveals the presence of crystalline Co_3O_4 phase of cubic system (JCPDS No: 43-1003). The Co_3O_4/KB (80%) film shows no crystalline peaks of Co_3O_4 except the sharp peaks of foam Ni and a broad peak around 20-25^o attributed to KB, which may be resulted from the small amount of Co_3O_4 wrapped by KB clusters (Fig. 3b). XPS spectrum of Co_3O_4/KB (80%) was conducted to confirm the existence of Co_3O_4 in the composite. The high resolution XPS spectrum of Co 2p of the sample is shown in Fig. 3c. After fitted with Gaussian-Lorentzian (GL) functions, two separated peaks appear at 779.93 eV and 781.73 eV corresponding to Co^{3+} and Co^{2+} at the position of Co $2p_{3/2}$, while two

separated peaks appear at 795.13 eV and 797.15 eV corresponding to Co^{3+} and Co^{2+} at the position of Co $2p_{1/2}$. Besides, both peaks for Co $2p_{3/2}$ and $2p_{1/2}$ are clearly accompanied by satellite structures on their higher binging energy side. All the results indicate the coexistence of Co^{2+} and Co^{3+}, which suggests the formation of Co_3O_4 in the as-deposited Co_3O_4/KB (80%).

We next evaluate the electrocatalytic effect of the Co_3O_4/KB on the electrochemical properties of a Li-O_2 cell. The O_2 electrodes were prepared and tested in the range of 2.0-4.3 V at a current density of 100 mA g^{-1}. The charge/discharge profiles of the electrodes with different percentage of KB at the first, second and third cycles are compared in Fig. 4. The Co_3O_4/KB (80%) electrode achieves the highest initial capacity of 2044 mA h g^{-1}, while Co_3O_4/KB (20%), Co_3O_4/KB (60%) and pure KB electrodes behave lower performances as 243mAh g^{-1}, 1243 mAh g^{-1} and 1729 mAh g^{-1}, respectively. After the first cycle, Co_3O_4/KB (20%) and Co_3O_4/KB (60%) keep a relatively stable performance but lower capacity, due to insufficient electric conductivity. The reversible discharge/charge capacity of Co_3O_4/KB (80%) remains almost the same as 2300 mAh g^{-1}, which is even a little higher than the initial discharge capacity after an activation process. Therefore, it could be concluded that the good electric conductivity of KB promotes the overall electrocatalytic performance of Co_3O_4 cathodes. We also noted that the discharge/charge capacity of pure KB cathode largely decreases to 1321 mAh g^{-1} at the third cycle, which reveals the deficiency of catalytic activity of pure KB cathodes. In this way, KB with limited catalytic activity mainly acts as conductive agent and Co_3O_4 catalyst plays an

important role in cycling stability of Li-O_2 cell. The enhanced electrocatalytic activity of Co_3O_4/KB (80%) cathode could be confirmed from the lowest average overpotential of less than 1.0 V between charge and discharge plateau (Fig. 4e), where the OER potential is largely decreased. The results are comparable to the reported noble metal based catalyst [27, 28]. The improved performance of Co_3O_4/KB (80%) with better cycling stability and smaller overpotential could be a consequence of a compromise between electric conductivity and catalytic activity.

Fig. 5a shows the cycling performance for the composites which were tested under a fixed cut-off capacity of 500 mAh g^{-1} at a current density of 100 mA g^{-1}. The Co_3O_4/KB (80%) performs the best cycle stability over 33 cycles, better than Co_3O_4/KB (60%) sustaining 24 cycles and KB keeping only 17 cycles. The result of Co_3O_4/KB (80%) is competitive among various transition metal oxide-based catalysts. Kang *et al.* reported TiO_2 nanofibers catalysts which facilitate reversible reactions over 10 cycles under limited capacity conditions (1000 mAh g^{-1}_{carbon})[29]. Hierarchical mesoporous γ-Fe_2O_3/carbon nanocomposites reported by Chen *et al.* show good cycle performance over 30 cycles with stable reversible capacities of 600 mAh g^{-1}[30]. The capacity retention of nanoporous NiO Plates sustains over 70 cycles demonstrated under a limited capacity of 1000 $mAhg^{-1}_{CNT}$[31]. MnO_2 catalysts, as one of the most popular cathode catalysts as Co_3O_4, were recently reported to keep over 30 cycles remaining little difference with a limited depth of discharge (500 $mAhg^{-1}$)[32]. The electrochemical performance in the present work is comparable among all these reports. Meanwhile, Fig. 5b shows the corresponding initial discharge

and charge voltage of cathodes with different content of KB calculated at 250 mA h g^{-1}. The results clearly indicate a sluggish kinetics of OER and ORR process either when Co_3O_4 catalyst is lacked or when conductive agent of KB occupies too little, corresponding that Co_3O_4/KB (20%) and pure KB at both ends show a much higher overpotential during charge and discharge processes.

The enhanced electrocatalytic performance of Co_3O_4/KB (80%) could be further evidenced by CV measurements in Fig. 6. Similar to the almost overlapped discharge voltage curves of all the cathodes in Fig. 4e, the initial reduction peak of Co_3O_4/KB (80%) and KB cathode locates at around the same position, but sharper shape and larger peak areas can be noted for Co_3O_4/KB (80%), which shows faster ORR kinetics during first discharge of Co_3O_4/KB (80%) over KB cathode. A significantly higher catalytic activity during OER for Co_3O_4/KB (80%) could be observed from the higher oxidation current following the discharge process. Interestingly, a three-stage behavior, hinted from three distinct peaks in cathodic scan, is observed in the initial charging process. Yang *et.al* has proposed a reaction mechanism of Li-O_2 battery to illuminate the recharge voltage profile presenting similar feature as our work. The hypothesize in their report stated that the OER associated with the initial recharge sloping period is attributed to a de-intercalation process via a solid-solution route from the outer part of Li_2O_2 to form LiO_2-like species on the surface ($Li_2O_2 \rightarrow LiO_2 + Li^+ + e^-$), where LiO_2-like species disproportionate to evolve O_2 ($LiO_2 + LiO_2 \rightarrow Li_2O_2 + O_2$). The OER process at the flat potential plateau can be attributed to the oxidation of bulk Li_2O_2 particles, which generates Li^+ ions and O_2 ($Li_2O_2 \rightarrow 2Li^+ + 2e^- + O_2$) via a

two-phase transition. Additionally, a rising charge plateau after the second stage has been assigned to the decomposition of carbonate-type byproducts and electrolyte [33]. In our work the three-stage behavior during charge process with three peaks at 3.2 V, 3.5 V and 4.1 V correspond to this reaction mechanism well. However, the pure KB cathode only shows a broad peak around 4.0 V which may result from some side reactions. The following two cycles largely sustained without obvious decline of peak area and increase of overpotential, which represent the best ORR and OER electrocatalytic activity occurred on the Co_3O_4/KB (80%) cathode.

Meanwhile, EIS analysis of Li-O_2 cell was conducted to investigate the resistance of these cathodes loaded with different concentration of conductive agent (Fig. 7). The Co_3O_4/KB (80%) cathode shows the minimum charge transfer resistance (R_{ct}) before cycle test, after 1^{st} discharge and 1^{st} charge, predicted by a much smaller semi-circular at high/medium frequency. Meanwhile the diffusion of lithium ions accelerate apparently in Li-O_2 cell with the Co_3O_4/KB (80%) cathode, as its Z'- Z'' curve is much steeper at low frequency, which shows a capacitor-like behavior. This rare phenomenon in lithium air batteries has not been reported before. More work is ongoing to elucidate this phenomenon. All fitted EIS data with equivalent circuit are listed in Table 1, all cathode materials present an amplified R_{ct} after insulate Li_2O_2 generated on the surface of cathode materials. However, Co_3O_4/KB (80%) cathode shows the slightest increase of R_{ct} which also indicates the best combination of electric conductivity and catalytic ability. In the following charge process, the R_{ct} of Co_3O_4/KB (80%) cathode decrease from 75 ohm to 59 ohm after discharge products

are removed from the surface, implying a high OER catalytic activity achieved under this optimized ratio of KB to Co_3O_4.

4. Conclusion

We optimized composite ratio of Li-O_2 catalyst to conductive agent to achieve the compromise of electric conductivity and catalytic activity. The Co_3O_4/KB (80%) cathode shows an enhanced Li-O_2 performance with the highest initial discharge specific capacity of 2044 mAh g^{-1} under a current density of 100 mA g^{-1}, the lowest over-potential of less than 1.0 V, and the most stable cyclability. When setting the maximum capacity to 500 mA h g^{-1}, the Co_3O_4/KB (80%) cathode keeps 33 cycles under a low overpotential. The high intrinsic electrocatalytic activity and fast kinetics of ORR and OER process within electrocatalyst Co_3O_4/KB (80%) are confirmed by CV and EIS test.

Acknowledgements

This work was supported by National Natural Science Foundation of China (NSFC-21373184) and Doctoral Fund of Ministry of Education of China.

References

[1] P.G. Bruce, L.J. Hardwick, K.M. Abraham, Lithium-air and lithium-sulfur batteries, MRS Bull. 36 (2011) 506-512.

[2] J. Lu, L. Li, J.-B. Park, Y.-K. Sun, F. Wu, K. Amine, Aprotic and Aqueous Li-O_2 Batteries, Chem. Rev. 114 (2014) 5611-5640.

[3] F. Li, T. Zhang, H. Zhou, Challenges of non-aqueous Li–O_2 batteries: electrolytes, catalysts, and anodes, Energy Environ. Sci. 6 (2013) 1125.

[4] P.G. Bruce, S.A. Freunberger, L.J. Hardwick, J.-M. Tarascon, Li-O_2 and Li-S batteries with high energy storage, Nat. Mater. 11 (2012) 19-29.

[5] F.J. Li, T. Zhang, H.S. Zhou, Challenges of non-aqueous Li-O_2 batteries: electrolytes, catalysts, and anodes, Energy Environ. Sci. 6 (2013) 1125-1141.

[6] Y.Y. Shao, F. Ding, J. Xiao, J. Zhang, W. Xu, S. Park, J.G. Zhang, Y. Wang, J. Liu, Making Li-Air Batteries Rechargeable: Material Challenges, Adv. Funct. Mater. 23 (2013) 987-1004.

[7] B. Horstmann, B. Gallant, R. Mitchell, W.G. Bessler, Y. Shao-Horn, M.Z. Bazant, Rate-Dependent Morphology of Li_2O_2 Growth in Li-O_2 Batteries, J. Phys. Chem. Lett. 4 (2013) 4217-4222.

[8] M. Leskes, A.J. Moore, G.R. Goward, C.P. Grey, Monitoring the Electrochemical Processes in the Lithium-Air Battery by Solid State NMR Spectroscopy, J. Phys. Chem. C 117 (2013) 26929-26939.

[9] H.D. Lim, H. Song, H. Gwon, K.Y. Park, J. Kim, Y. Bae, H. Kim, S.K. Jung, T. Kim, Y.H. Kim, X. Lepro, R. Ovalle-Robles, R.H. Baughman, K. Kang, A new catalyst-embedded hierarchical air electrode for high-performance Li-O_2 batteries, Energy Environ. Sci. 6 (2013) 3570-3575.

[10] Z.L. Jian, P. Liu, F.J. Li, P. He, X.W. Guo, M.W. Chen, H.S. Zhou, Core-Shell-Structured CNT@RuO_2 Composite as a High-Performance Cathode Catalyst for Rechargeable Li-O_2 Batteries, Angew. Chem., Int. Ed. 53 (2014) 442-446.

[11] B.M. Gallant, R.R. Mitchell, D.G. Kwabi, J. Zhou, L. Zuin, C.V. Thompson, Y. Shao-Horn, Chemical and Morphological Changes of Li-O_2 Battery Electrodes upon Cycling, J. Phys. Chem. C 116 (2012) 20800-20805.

[12] T. Ogasawara, A. Debart, M. Holzapfel, P. Novak, P.G. Bruce, Rechargeable Li2O2 electrode for lithium batteries, J. Am. Chem. Soc. 128 (2006) 1390-1393.

[13] Z. Zhang, J. Lu, R.S. Assary, P. Du, H.-H. Wang, Y.-K. Sun, Y. Qin, K.C. Lau, J. Greeley, P.C. Redfern, H. Iddir, L.A. Curtiss, K. Amine, Increased Stability Toward Oxygen Reduction Products for Lithium-Air Batteries with Oligoether-Functionalized Silane Electrolytes, J. Phys. Chem. C 115 (2011) 25535-25542.

[14] R.S. Assary, K.C. Lau, K. Amine, Y.-K. Sun, L.A. Curtiss, Interactions of Dimethoxy Ethane with Li_2O_2 Clusters and Likely Decomposition Mechanisms for Li-O_2 Batteries, J. Phys. Chem. C 117 (2013) 8041-8049.

[15] Z. Peng, S.A. Freunberger, Y. Chen, P.G. Bruce, A Reversible and Higher-Rate Li-O_2 Battery, Science 337 (2012) 563-566.

[16] Y.-C. Lu, Z. Xu, H.A. Gasteiger, S. Chen, K. Hamad-Schifferli, Y. Shao-Horn, Platinum-Gold Nanoparticles: A Highly Active Bifunctional Electrocatalyst for Rechargeable Lithium-Air Batteries, J. Am. Chem. Soc. 132 (2010) 12170-12171.

[17] B. Sun, P. Munroe, G. Wang, Ruthenium nanocrystals as cathode catalysts for lithium-oxygen batteries with a superior performance, Sci. Rep. 3 (2013) 2247.

[18] D. Oh, J.F. Qi, B.H. Han, G.R. Zhang, T.J. Carney, J. Ohmura, Y. Zhang, S.H. Yang, A.M. Belcher, M13 Virus-Directed Synthesis of Nanostructured Metal Oxides for Lithium-Oxygen Batteries, Nano Lett. 14 (2014) 4837-4845.

[19] Y.M. Cui, Z.Y. Wen, Y. Liu, A free-standing-type design for cathodes of rechargeable Li-O_2 batteries, Energy Environ. Sci. 4 (2011) 4727-4734.

[20] C.W. Sun, F. Li, C. Ma, Y. Wang, Y.L. Ren, W. Yang, Z.H. Ma, J.Q. Li, Y.J. Chen, Y. Kim, L.Q. Chen, Graphene-Co_3O_4 nanocomposite as an efficient bifunctional catalyst for lithium-air batteries, J. Mater. Chem. A 2 (2014) 7188-7196.

[21] A. Riaz, K.N. Jung, W. Chang, S.B. Lee, T.H. Lim, S.J. Park, R.H. Song, S. Yoon, K.H. Shin, J.W. Lee, Carbon-free cobalt oxide cathodes with tunable nanoarchitectures for rechargeable lithium-oxygen batteries, Chem. Commun. 49 (2013) 5984-5986.

[22] G.Y. Zhao, Z.M. Xu, K.N. Sun, Hierarchical porous Co_3O_4 films as cathode catalysts of rechargeable Li-O_2 batteries, J. Mater. Chem. A 1 (2013) 12862-12867.

[23] A. Debart, J. Bao, G. Armstrong, P.G. Bruce, An O_2 cathode for rechargeable lithium batteries: The effect of a catalyst, J. Power Sources 174 (2007) 1177-1182.

[24] C.S. Park, K.S. Kim, Y.J. Park, Carbon-sphere/Co_3O_4 nanocomposite catalysts for effective air electrode in Li/air batteries, J. Power Sources 244 (2013) 72-79.

[25] W.H. Ryu, T.H. Yoon, S.H. Song, S. Jeon, Y.J. Park, I.D. Kim, Bifunctional Composite Catalysts Using Co_3O_4 Nanofibers Immobilized on Nonoxidized Graphene Nanoflakes for High-Capacity and Long-Cycle Li-O_2 Batteries, Nano Lett. 13 (2013) 4190-4197.

[26] T.H. Yoon, Y.J. Park, Polydopamine-assisted carbon nanotubes/Co_3O_4 composites for rechargeable Li-air batteries, J. Power Sources 244 (2013) 344-353.

[27] Y.-C. Lu, H.A. Gasteiger, E. Crumlin, R. McGuire, Jr., Y. Shao-Horn, Electrocatalytic Activity Studies of Select Metal Surfaces and Implications in Li-Air Batteries, J. Electrochem. Soc. 157 (2010) A1016-A1025.

[28] F. Li, Y. Chen, D.-M. Tang, Z. Jian, C. Liu, D. Golberg, A. Yamada, H. Zhou, Performance-improved Li-O_2 battery with Ru nanoparticles supported on binder-free

multi-walled carbon nanotube paper as cathode, Energy Environ. Sci. 7 (2014) 1648-1652.

[29] S.H. Kang, K. Song, J. Jung, M.R. Jo, Y.-M. Kang, Polymorphism-induced catalysis difference of TiO_2 nanofibers for rechargeable Li-O_2 batteries, J. Mater. Chem. A 2 (2014) 19660-19664.

[30] W. Chen, Z. Zhang, W. Bao, Y. Lai, J. Li, Y. Gan, J. Wang, Hierarchical mesoporous gamma-Fe_2O_3/carbon nanocomposites derived from metal organic frameworks as a cathode electrocatalyst for rechargeable Li-O_2 batteries, Electrochim. Acta 134 (2014) 293-301.

[31] M. Hong, H.C. Choi, H.R. Byon, Nanoporous NiO Plates with a Unique Role for Promoted Oxidation of Carbonate and Carboxylate Species in the Li–O_2 Battery, Chem. Mater. 27 (2015) 2234-2241.

[32] P. Zhang, M. He, S. Xu, X. Yan, The controlled growth of porous delta-MnO_2 nanosheets on carbon fibers as a bi-functional catalyst for rechargeable lithium-oxygen batteries, J. Mater. Chem. A 3 (2015) 10811-10818.

[33] Y.-C. Lu, Y. Shao-Horn, Probing the Reaction Kinetics of the Charge Reactions of Nonaqueous Li-O_2 Batteries, J. Phys. Chem. Lett. 4 (2013) 93-99.

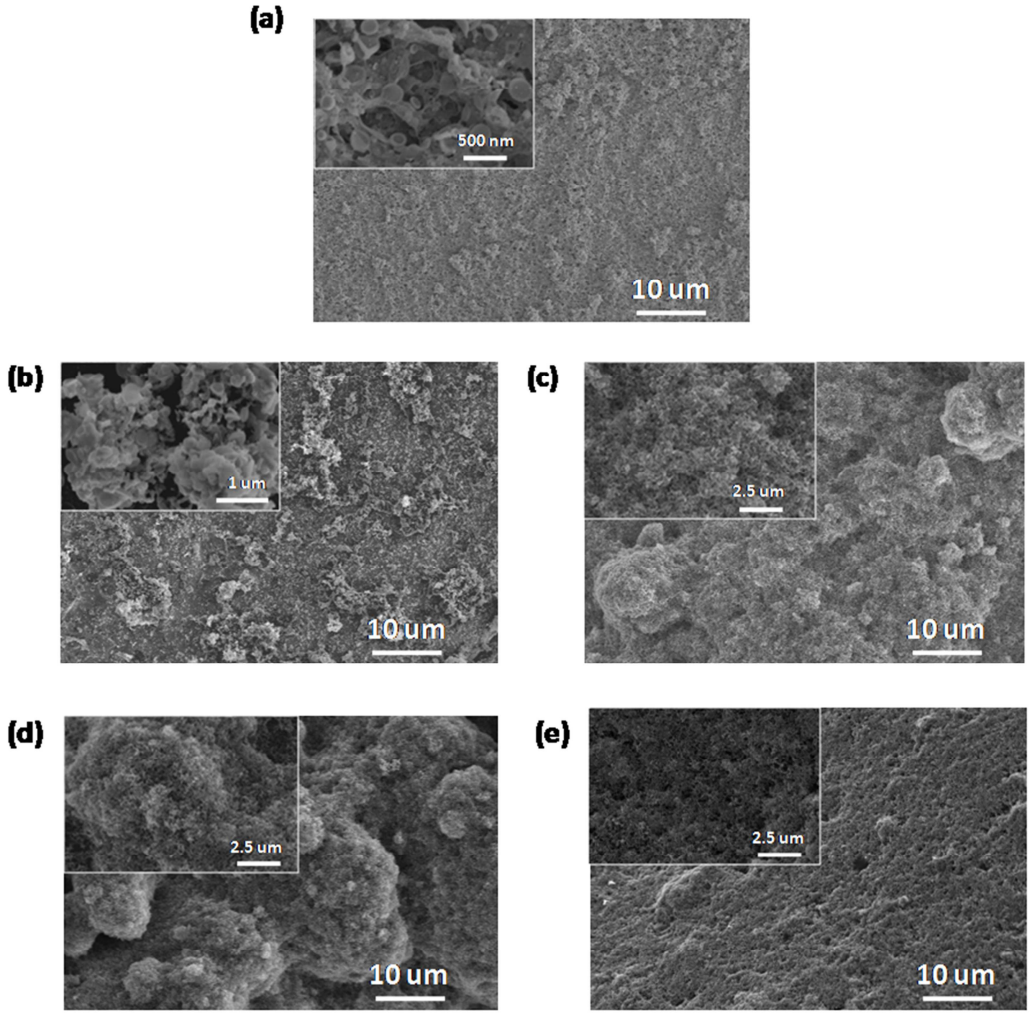

Fig. 1 SEM images of as-deposited electrodes, **a)** pure Co_3O_4, **b)** Co_3O_4/KB (20%), **c)** Co_3O_4/KB (60%), **d)** Co_3O_4/KB (80%), **e)** pure KB.

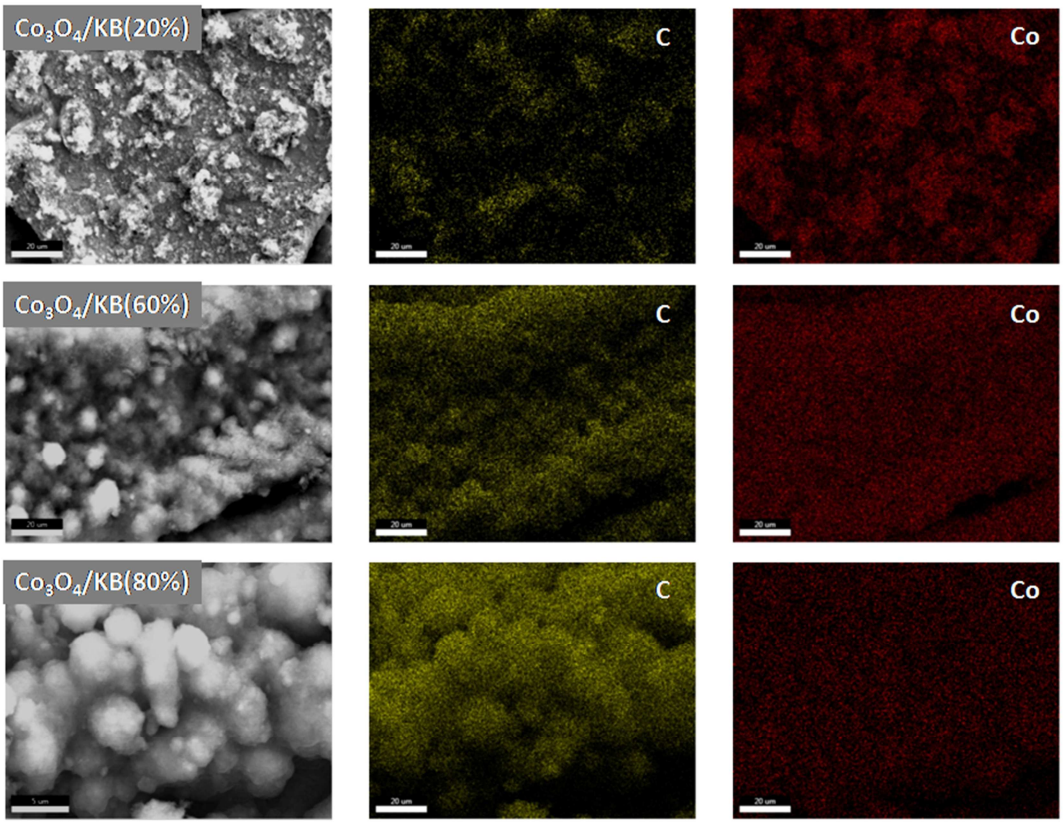

Fig. 2 EDS mapping of the element Co and C of the as-deposited electrodes of Co_3O_4/KB (20%), Co_3O_4/KB (60%) and Co_3O_4/KB (80%).

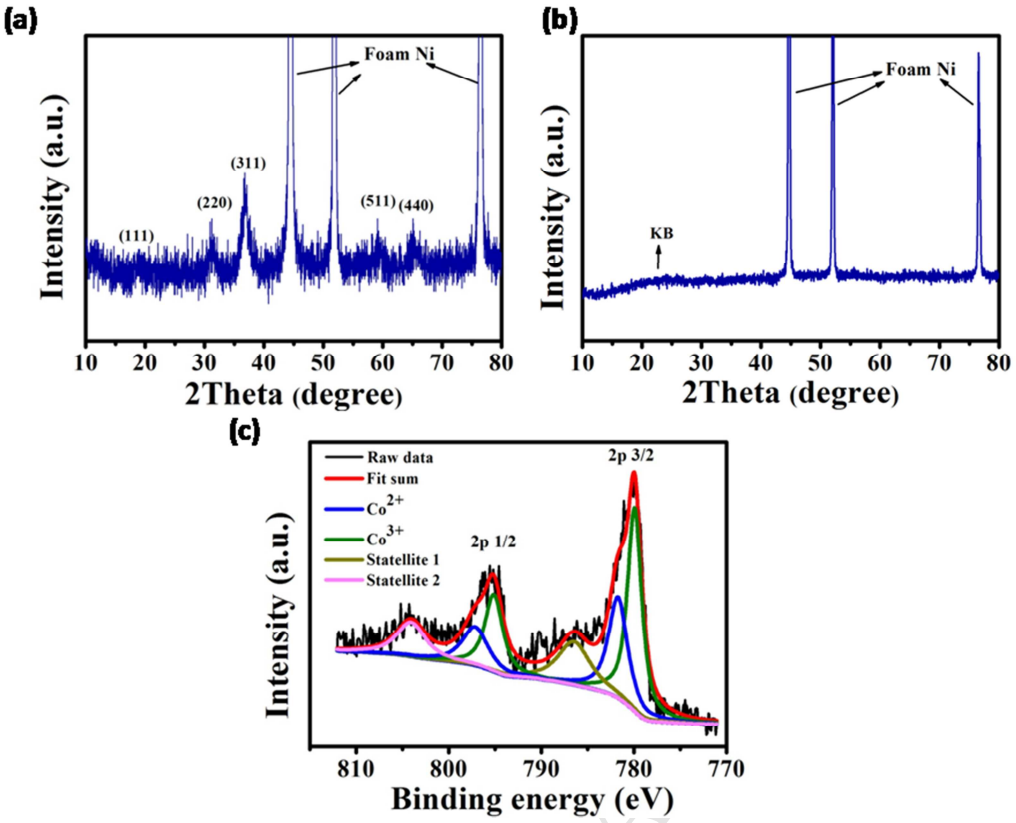

Fig. 3 XRD patterns of **a)** pure Co_3O_4, **b)** Co_3O_4/KB (80%) electrode.**c)** XPS spectrum of the element Co in Co_3O_4/KB (80%) electrode.

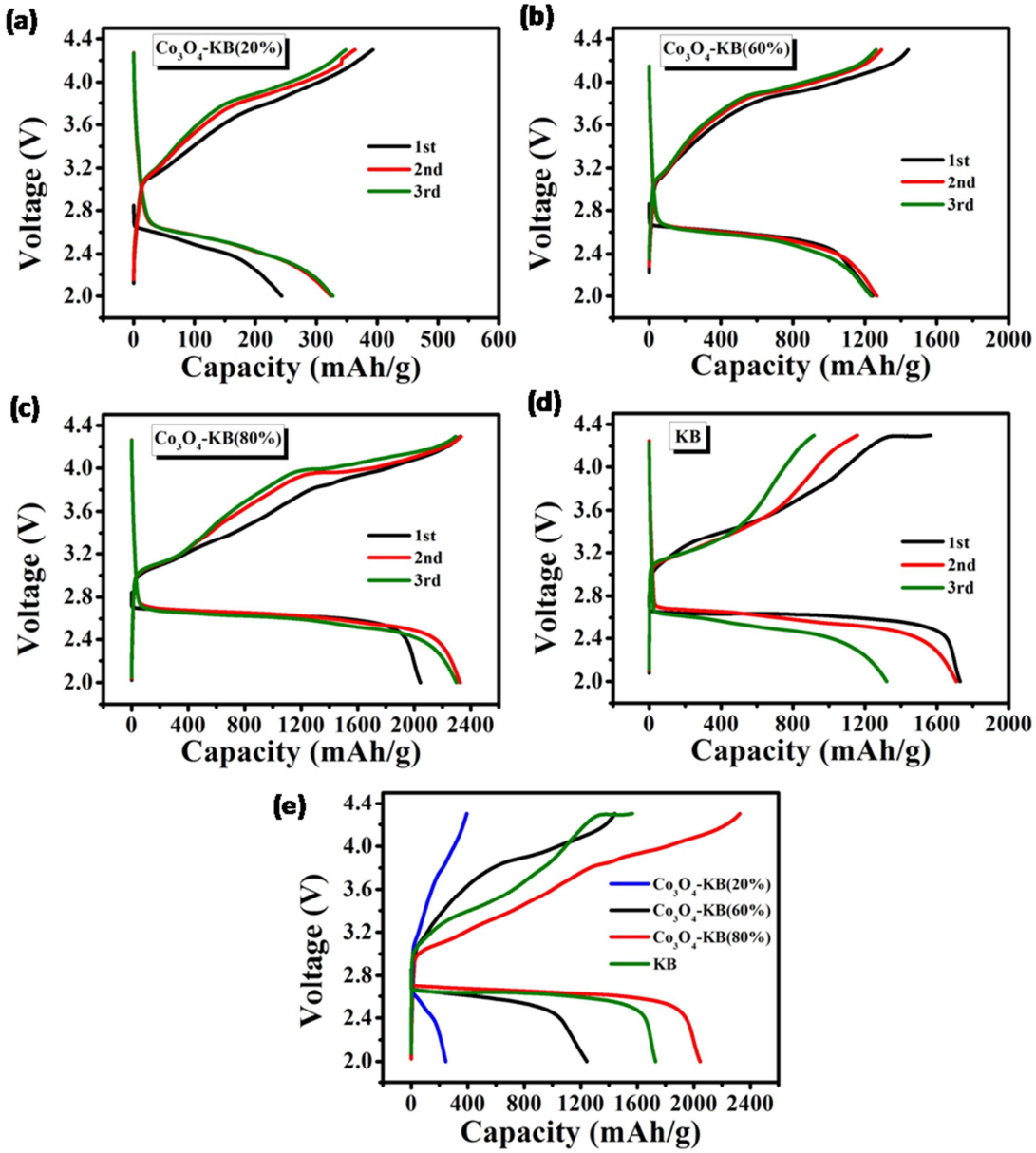

Fig. 4 Charge and discharge profiles of **a)** Co_3O_4/KB (20%), **b)** Co_3O_4/KB (60%), **c)** Co_3O_4/KB (80%), **d)** pure KB electrodes. **e)** Direct comparison between initial charge-discharge voltage curves of these electrodes. All the cells are operated under the current density of 100 mA g^{-1} from 2.0-4.3 V.

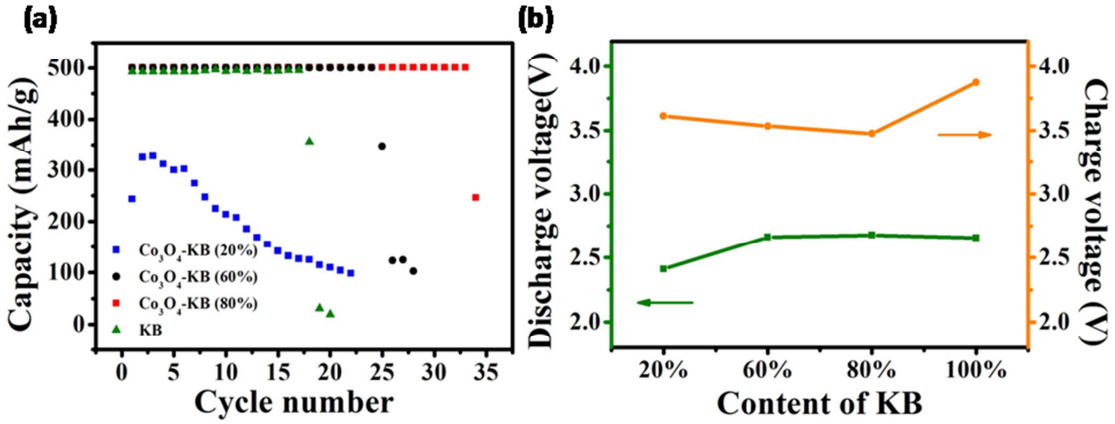

Fig. 5 a) Cycle performance of cathodes with different content of KB with curtailing the capacity to 500 mAh g^{-1} under the current density of 100 mA g^{-1}, **b)** the corresponding charge and discharge voltage measured at half the capacity in left figure.

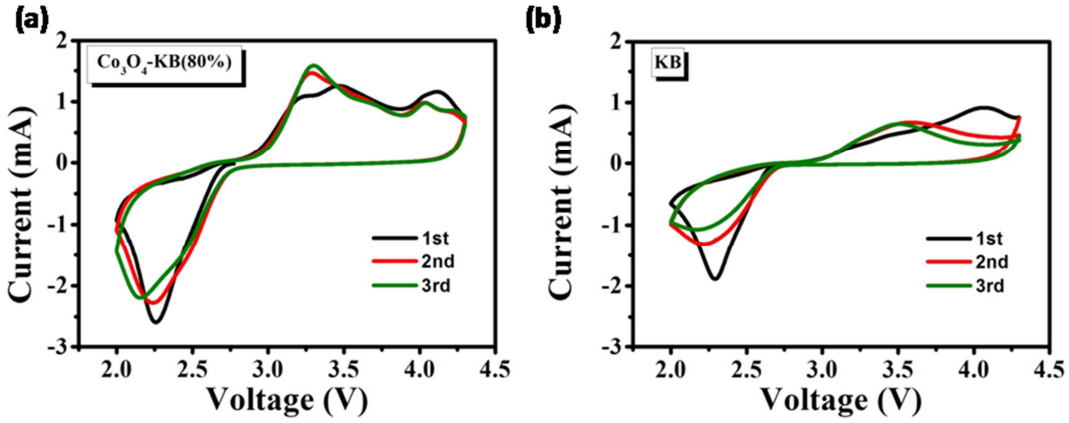

Fig. 6 CV curve results of initial 3 cycles of **a)** Co_3O_4/KB(80%), **b)** KB electrodes at a constant scan rate at 0.5mV s^{-1} from 2.0-4.3 V.

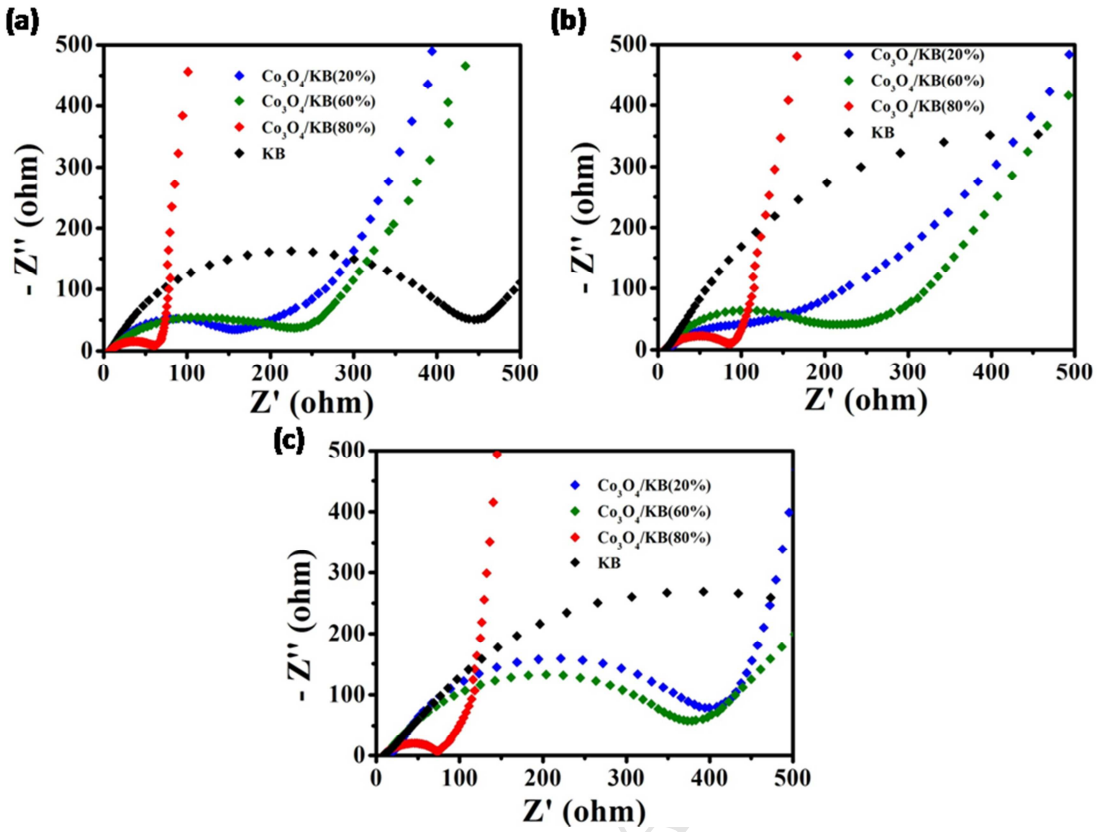

Fig. 7 EIS analysis of Co_3O_4/KB (20%), Co_3O_4/KB (60%), Co_3O_4/KB (80%) and pure KB electrodes of Li-O_2 cell, **a)** before cycle test, **b)** after 1st discharge, **c)** after 1st charge.

Table 1 The best fit values of EIS data with equivalent circuit of electrodes in Fig. 7.

R_{ct} (ohm)	Before cycle	After 1st discharge	After 1st charge
Co_3O_4/KB (20%)	160	497	87
Co_3O_4/KB (60%)	179	166	308
Co_3O_4/KB (80%)	53	75	59
KB	387	790	398

Highlights:

- A series of Co_3O_4/KB composites cathodes in lithium oxygen batteries were prepared.
- Co_3O_4/KB (80%) shows largest capacity, lowest overpotential and best stability.
- The relationship of electrical conductivity and catalytic activity is studied.